SCIENTIFIC REPORTS

OPEN

SUBJECT AREAS:
MINERALOGY
THEORY AND COMPUTATION

Received
11 June 2014

Accepted
9 January 2015

Published
6 March 2015

Correspondence and requests for materials should be addressed to A.Z. (azaoui@polytech-lille.fr)

Can clays ensure nuclear waste repositories?

A. Zaoui & W. Sekkal

Civil Engineering and geo-Environment Laboratory LGCgE- (EA 4515) Lille Nord de France, Polytech'Lille, Université des Sciences et de la Technologie de Lille. Cité Scientifique, Avenue Paul Langevin, 59655 Villeneuve D'Ascq Cedex, France.

Research on argillite as a possible host rock for nuclear waste disposal is still an open subject since many issues need to be clarified. In the Underground Research Laboratories constructed for this purpose, a damaged zone around the excavation has been systematically observed and characterized by the appearance of micro-fissures. We analyse here -at nanoscale level- the calcite/clay assembly, the main constituents of argillite, under storage conditions and show the fragility of the montmorillonite with respect to calcite. Under anisotropic stress, we have observed a shear deformation of the assembly with the presence of broken bonds in the clay mineral, localised in the octahedral rather than the tetrahedral layers. The stress/strain curve leads to a failure strength point at 18.5 MPa. The obtained in-plane response of the assembly to perpendicular deformation is characterized by smaller perpendicular moduli E_z = 48.28 GPa compared to larger in-plane moduli E_x = 141.39 GPa and E_y = 134.02 GPa. Our calculations indicate the instability of the assembly without water molecules at the interface in addition to an important shear deformation.

The choice of mineral rocks for the isolation of the High-Level radioactive wastes is still a challenge and considered as the most reliable and technically feasible way in deep geological disposal in many countries[1–7]. For the French high-level nuclear waste, the Callovo-Oxfordian argillite is considered as a possible host rock at great depth[8]. It is a geological clay layer with a very low permeability and a good ability to retain radionuclides by physico-chemical adsorption. It is a stiff sedimentary rock, deform with time but very slowly[9–14]. From a mineralogical point of view[8] (Fig. 1), the Callovo-Oxfordian argillite is mainly composed of four groups whose proportions vary in the thickness of the stratigraphic layer (i) clay minerals consist mainly of a mixture of illite and interstratified illite/smectite (20–60%), (ii) tectosillicates mainly quartz (10–40%), (iii) carbonate, calcite principally (10–75%) and dolomite (2–8%) and (iv) so-called "heavy" mineral, mainly pyrite (0,5–1%) and siderite (0.5–3%).

A repository constitutes a complex system whose evolution depends on various phenomena (thermal, hydraulic, chemical and mechanical). The challenge is to build repositories that will remain stable and without any leaks for long periods of time. Among required characteristics is the plastic behavior that allows the system to deform without the formation of fissures.

In the Bure Underground Research Laboratory (URL) (in France), an excavation damaged zone (EDZ) is observed around galleries in the Callovo-Oxfordian argillite and is characterized by the appearance of micro-fissures whose density decreases as the distance from the wall increases (Fig. 2)[8]. At a depth of 517 m, the stress orientation is as: vertical stress ($\sigma_v \approx 12{,}7\ MPa$), minor horizontal stress ($\sigma_h \approx 12{,}7\ MPa$) and major horizontal stress ($\sigma_H \approx 16{,}5\ MPa$). Therefore, it is necessary and essential to understand what is behind this anisotropic damage with regard to the mechanical behaviour of the argillite under various phenomena (thermal, hydraulic and chemical). From the microscopic point of view, the local cracking and failure of repositories always generate acoustic emission (AE) signals. The AE monitoring technology, one of the most efficient way to monitor the failure locations, can improve the safety performance of the structure of repositories. AE localisations gave us an image of the pre- and post-failure localisation, Dong et al.[15–18] have conducted original works with deriving some analytic/optimized solutions to locate AE signals. These research results can be used to monitor and evaluate fissures of repositories. Changes in acoustic emissions (AE) and elastic wave velocities were monitored by P-wave and S-polarized piezoelectric sensors. These acoustic velocities in a solid can be derived from the bulk (B) and shear (G) moduli of the material, as well as the density ρ.

The purpose of this study is to use the nanoscale tools to analyse the disturbed zone at the atomic level in order to see the different processes responsible for this behaviour. As the main constituents of argillite are clay and calcite, attention will be paid to the interaction between these two rocks under storage conditions. Molecular dynamics simulations have been performed in NPT ensemble using time step of 1 femtosecond. Internal energy

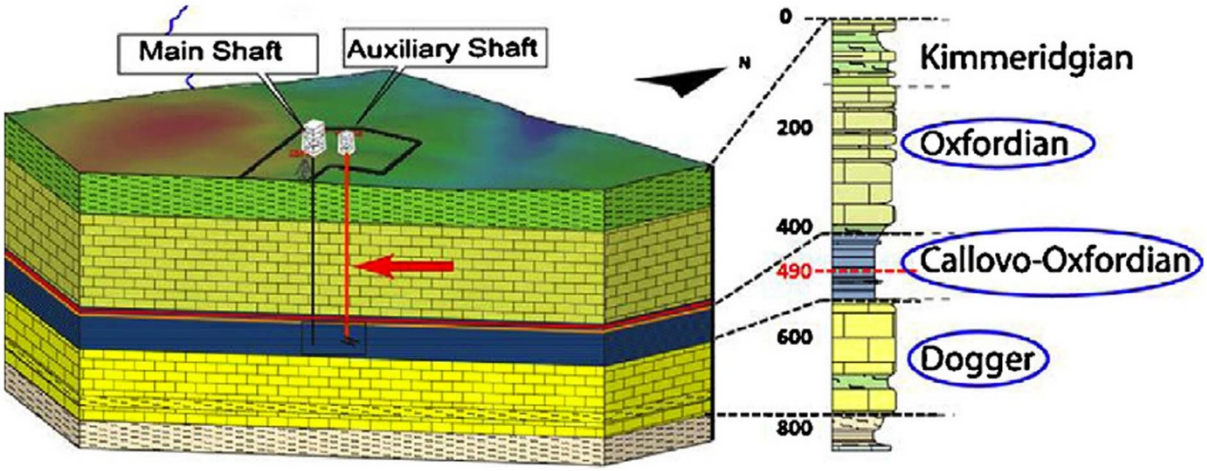

Figure 1 | **Sedimentary sequence in the Paris Basin, with indication of the Bure underground research laboratory in the Callovo-Oxfordian argillite (clay) formation.**

minimizations are performed allowing all individual ionic coordinates and lattice parameters to vary. In this study, we analyse, first, the behaviour of the montmorillonite (001)/calcite (104) interface under the effect of anisotropic stress at a fixed temperature of 90°. In the second experience, we apply a shear stress (xy, xz and yz) to the assembly. These simulations are carried out in the presence of water at the interface.

In the first experience, we have applied an anisotropic stress to the calcite/clay interface with σ_{xx} = 13 MPa, σ_{yy} = 16.9 MPa, while the vertical stress σzz varies from 0 to 20 MPa. For each value of σ_{zz}, we compress the assembly then we release the constraint and leave the system to relax. The obtained stress/strain response is shown in Fig. 3a.

We notice that the deformation of the assembly is anisotropic, more pronounced along the vertical direction. This anisotropy is caused by compression of the interlayer space along the z direction, which requires much smaller forces than the compression of aluminosilicate layers in-plane. The in-plane response of the assembly to perpendicular deformation is characterized by smaller perpendicular moduli E_z (48.28 GPa) compared to larger in-plane moduli (E_x = 141.39 GPa, E_y = 134.02 GPa). Thus the ratio (the perpendicular moduli over the in-plane moduli) is equal to 2.8. This value is in agreement with the experimental measurement of the anisotropic ratio of the Young's modulus, which is equal to 2[19]. This explains the easier deformation of the assembly along z direction rather than the horizontal one (more resistance to deformation).

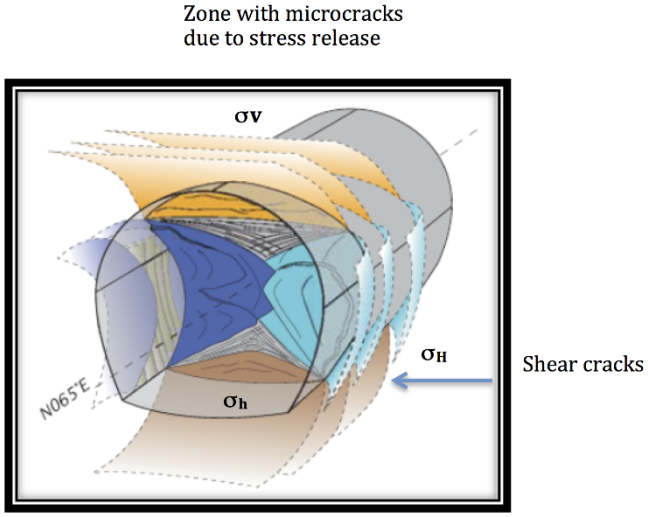

Figure 2 | **Damaged zone around the excavation[8].**

As shown in Fig. 3a, the stress/strain curves deal with three phases: elastic, plastic and a failure phase. The obtained failure strength corresponds to 18.5 MPa for both the vertical and the horizontal direction. We have observed that the plastic behaviour of the assembly is obtained when the vertical stress σzz varies between 18 and 20 MPa. The corresponding strains variations are: from 0.02 to 0.04 along x direction, betwwen 0.05 and 0.1 along y direction and between 0.08 and 0.13 along the vertical direction. These can be the conditions to have a deformation of the assembly without the formation of fissures.

Previous hierarchical simulation techniques at the electronic and atomistic levels show the strength and possible failure mechanisms of Layered Silicates over the range of cation densities[20]. Their study on pyrophylite, montmorillonite and mica showed a large mechanical anisotropy, kinks, cation intrusion, and shear flow in the aluminosilicate layers. Besides intense research efforts have been dedicated to the mechanical properties of clay minerals on the macroscale[21–30].

We present in Fig. 3b the relaxed atomistic assembly after the application of the storage stress conditions (σ_{xx} = 13 MPa, σ_{yy} = 16.9 MPa and σ_{zz} = 13.4 MPa). We observe, first, that the damage is present in the clay layers part and not in calcite. These broken bonds (in the clay layers) are noticed in the octahedral rather than the tetrahedral layers. We note that the bonding distances of Si-O and Al-O are 1.58 Å and 1.98 Å, respectively, which could explain the difficulty to break the tetrahedral bond. Moreover, we observe from Fig. 3b that the assembly has a shear deformation.

In Fig. 4, we plot the variation of the interfacial distance and the thickness of the first interlayer depending on the vertical stress. It appears that under the application of a vertical constraint between 5 MPa and 13.4 MPa, the thickness of the clay layer increases by 1.39 Å, while the interfacial distance undergoes a slight increase (0.42 Å). Besides, when applying a stress from 13.4 MPa to 18.5, the clay layer undergoes a slight compression of 0.38 Å, while the interfacial distance decreases with 0.30 Å. From 18 MPa to 20 MPa, the thickness of the interlayer layer increases rapidly with 1.63 Å; for the interfacial distance it undergoes a sudden compression of 1.21 Å.

Regarding the response of the interface to the vertical deformation, we remark that, in the presence of water molecules at the interface, (see Fig. 5a and b) no damage is observed nether in the tetrahedral clay layer nor in the calcium carbonate one. Furthermore we noticed a slight shear deformation of the alumino-silicate as well as in calcium carbonate layers.

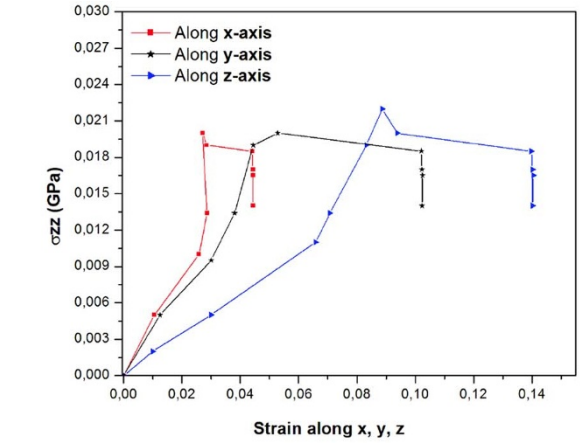

(a)

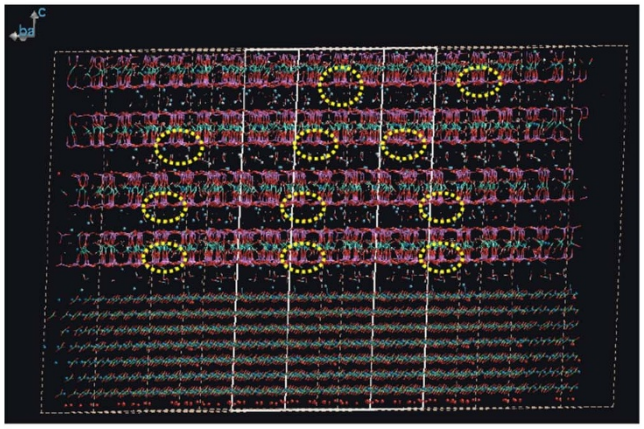

(b)

Figure 3 | (a): Stress/strain curve of the calcite/Montmorillonite assembly under storage conditions. (b) atomistic representation of the assembly after relaxation.

In Fig. 5b, we plot the relaxed interface of the assembly without water molecules (at the interface) after the application of anisotropic stress. We clearly observe the presence of broken bonds in the first

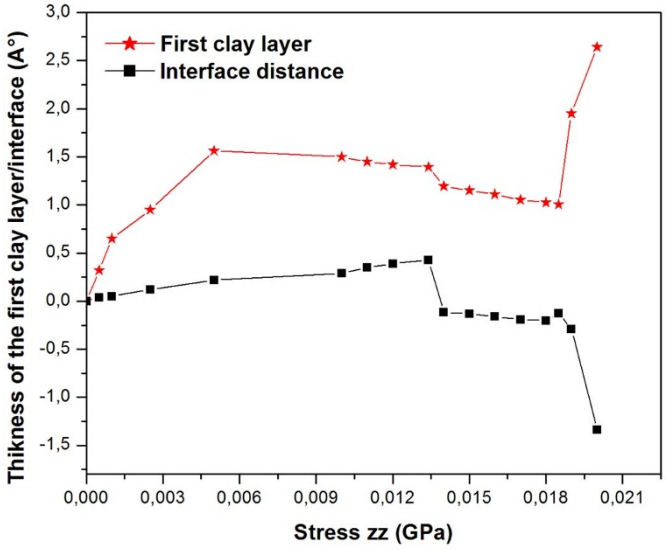

Figure 4 | **Variation of the thikness of the first clay layer and interfacial distance versus vertical stress.**

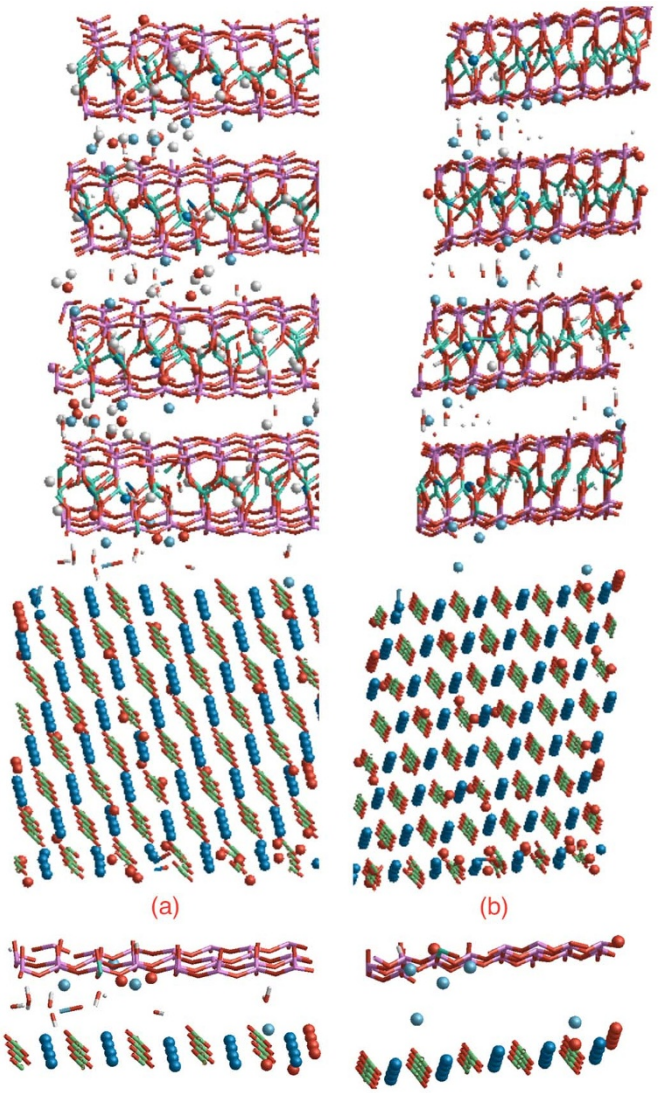

Figure 5 | Relaxed calcite/clay assembly: (a) with the presence of water molecules at the interface, (b) without water molecules at the interface.

tetrahedral clay layer. Note that the shear deformation in the clay layers is more pronounced in the case of an assembly without water at the interface. Our calculations show the instability of the assembly in the last case (without water at the interface) with a total energy of 27 680 eV and an expansion of the system about 0.7%.

We have already studied the water role in our recent work[31]. From the variation of the total energy versus the interfacial distance, we have shown that the presence of water has the effect of absorbing the excess energy provided by the system and thereby stabilize the interface. We note that our study of calcite/clay interface with the presence of water is the first work in such area. However, there are many other papers interested into the role of water on calcite surface. Experimental studies have given considerable information concerning the structure of the carbonate-water interface[32] and the growth mechanisms[33–34]. Other computational calculations have shown that the incorporation of water into the amorphous calcium carbonate nanoparticles make the system thermodynamically more stable[35]. Using a new force field, Raiteri et al.[36] have examined the thermodynamics of calcium carbonate-water system.

Responses to shear stress in the presence of water molecules at the interface were analysed in Fig. 6 in the xy, xz and yz planes. We remark that the assembly is more resistant to shear in the xy and xz planes compared to yz plane. Besides, we noticed that the system

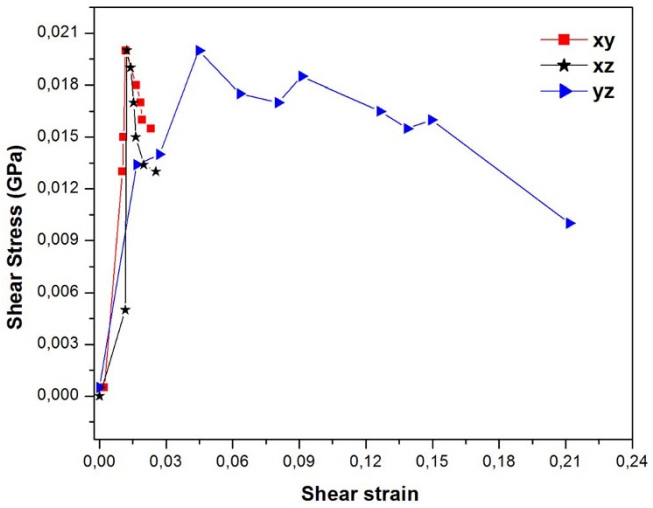

Figure 6 | **shear stress/strain curve for the xy, xz and yz planes.**

goes fastly to break and the obtained failure strength corresponds to 20 MPa. In Fig. 7, we present the relaxed system for a shear stress of 13.4 MPa and 17 MPa applied to xz plane. We have found that the system deforms without breaks for a shear stress equal to 13.4, while for 17 MPa, the assembly is unstable with the presence of broken bonds in the clay layers.

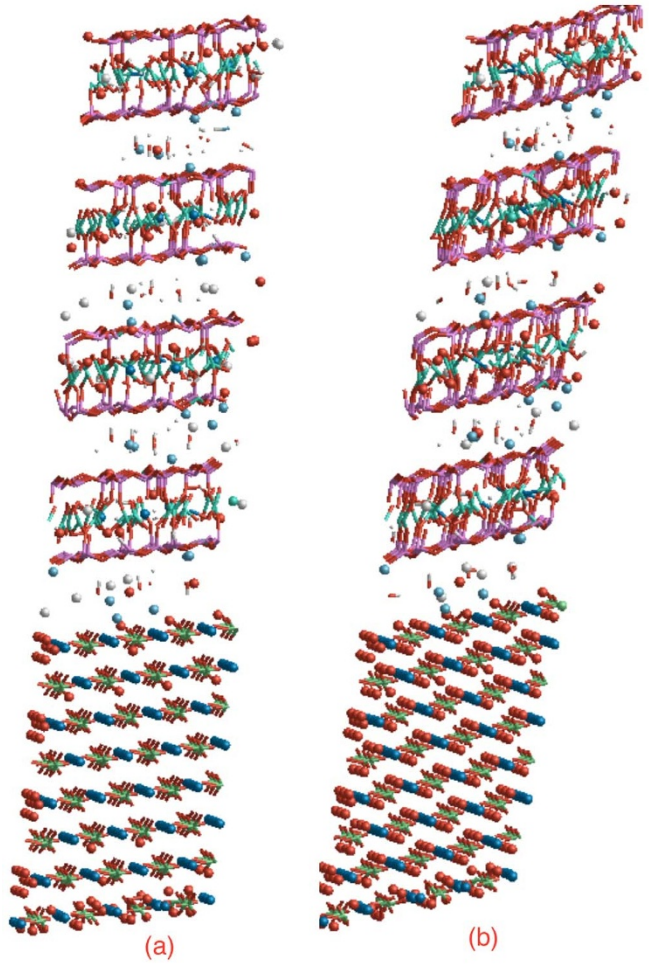

Figure 7 | Assembly under shear stress at: (a) 13.4 MPa and (b) 17 MPa applied to xz plane.

In summary, a nanoscale tool is used to analyse at the atomic level the mechanical behaviour of the calcite/clay interface under storage conditions. The assembly of the calcite (104) with montmorillonite (001) subject to storage conditions showed the fragility of the montmorillonite with respect to calcite, which resist to these conditions. The assembly calcite/clay is more deformable in the direction perpendicular to the interface (z-direction), which is due to the lamellar clays structure. Moreover, when applying an anisotropic stress, a failure point appears at 18.5 MPa with a compression of the interlayer space leading the breaks of the aluminosilicate bonds, which explains the damage around galleries in the Callovo- Oxfordian argillite. We have concluded that the presence of water molecules give more stability of the assembly since no damage at the interface has been observed in the tetrahedral clay layer nether in calcium carbonate part. Therefore, it is necessary to intensify studies on other mineral rocks, which do not lead damage under storage conditions and hence ensure the safety of nuclear waste repository.

Methods summary

To ensure a good accommodation at the interface, we built what we call the "supercell" by duplicating the unit cell of calcite 11 times in the x direction and 4 times in the y direction. For clay system, we duplicate the unit cell 3 times in the x direction and 5 times in the y direction. Therefore, the obtained lattice mismatch is 1.58% for the x direction and 2.9% for the y direction. Thus, the dimension of the simulation box is (5.53 × 10.39 × 70.50) nm, and $\alpha = 90^{\circ}$, the number of atoms is 26 280.

Potential model for the clay/calcite interface: The clay mineral model considered here is a Wyoming-type Montmorillonite, with the unit cell formula $Na_{0.75}[Si_{7.75}Al_{0.25}](Al_{3.5}Mg_{0.5})O_{20}(OH)_4{\cdot}nH_2O$. To describe the Montmorillonite (001)/calcite (104) interface, we have developed existing models for calcite and clay by adding terms describing the interatomic interactions between constituents of calcite and clay at the interface. We have used the ClayFF potential model[37], well tested for clays[38–49] and the Xiao forcefield for calcite[50], that we have previously used in the analysis of bulk and surface state of calcite rock[51]. This is a new forcefield taking into account the aqueous environment using the TIP3P water model[52]. At the interface, we have described the interactions between the last layer of the calcite (Ca^{2+}, CO_3^{2+}) and the first layer of clay (SiO_2) using the model of Guillot-Sator[53].

1. Lidskog, R. & Andersson, A. The management of radioactive waste A description of ten countries. *Other SKB reports* **ISBN-91-973987-3-X**, 1–107 (2002).
2. Kwon, S. Cho, W. J. & Lee, J. O. An analysis of the thermal and mechanical behavior of engineered barriers in a high-level radiactive waste repository. *Nuclear Eng. And Technol.* **45**, 41–52 (2013).
3. Madsen, F. T. Clay mineralogical investigations related to nuclear waste disposal. *Clay Miner.* **33**, 109–129 (1998).
4. Pusch, R. Use of bentonite for isolation of radioactive waste products. *Clay Miner.* **27**, 353–361 (1992).
5. Bish, D. L. Smectite Dehydration and Stability: Applications to Radioactive Waste Isolationat Yucca Mountain, Nevada. *Los Alamos National Laboratory report* LA-**11023**-*MS*, 31 (1988).
6. Holmboe, M., Jonsson, M. & Wold, S. Influence of γ-radiation on the reactivity of montmorillonite towards H_2O_2. *Radiation Phys. and Chem.* **81**, 190–194 (2012).
7. Takazawa, M. Experimental and modeling study to predict long-term alteration of bentonite buffer materials with alkaline groundwater. *JAERI-Conf* **7**, 236–341 (2005).
8. Armand, G., Noiret, A., Zghondi, J. & Seyedi, D. M. Short- and long-term behaviors of drifts in the Callovo-Oxfordian claystone at the Meuse/Haute-Marne Underground Research Laboratory. *J. Rock Mech. and Geotech. Eng.* **5**, 221 (2013).
9. Delage, P. Clays in radioactive waste disposal. *J. Rock Mech. and Geotech. Engineer.* **2**, 111–123 (2010).
10. Schlegel, M. L. *et al.* Metal corrosion and argillite transformation at the water-saturated, high-temperature iron–clay interface: A microscopic-scale study. *Geochem.* **23**, 2619–2633 (2008).
11. Ujiie, K., Tsutsumi, A., Fialko, Y. & Yamaguchi, H. Experimental investigation of frictional melting of argillite at high slip rates: Implications for seismic slip in subduction-accretion complexes. *J. of Geophys. Res.* **114**, 1–12 (2009).
12. Lassina, A. Equilibrium partial pressure of CO_2 in the Callovo-Oxfordian argillite as a function of relative humidity. *Procedia Earth and Planet. Sci.* **7**, 459–462 (2013).
13. Gaussen, J. L. Geological repository layout for radioactive high level long lived waste in argillite. *ENC Andra, INIS* **37**, 1–8 (2005).
14. Tang, C., Tang, A. M., Cui, Y. J., Delage, P. & Shi, B. The coupled hydro-mechanical behaviour of compacted crushed callovo-oxfordian argillite. *J. Rock Mech. and Geotech. Engineer.* **2**, 86–90 (2010).

15. Dong, L. J. & Li, X. B. Three-dimensional analytical solution of acoustic emission or microseismic source location under cube monitoring network. *Transactions of Nonferrous Metals Society of China* **22**, 3087–3094 (2012).
16. Dong, L. J. & Li, X. B. A microseismic/acoustic emission source location method using arrival times of PS waves for unknown velocity system. *Intern. J. of Distrib. Sensor Net.* **307489**, 1–8 (2013).
17. Dong, L. J., Li, X. B. & Xie. G. An analytical solution for acoustic emission source location for known P wave velocity system. *Math. Prob. in Engi.* **290686**, 1–6 (2014).
18. Dong, L. J. & Li, X. B. An efficient closed-form solution for acoustic emission source location in three-dimensional structures. *AIP Advances* **4**, 027110 (2014).
19. Armanda, G., Noireta, A., Zghondia, J. & Seyedi, D. M. Short- and long-term behaviors of drifts in the Callovo-Oxfordian claystone at the Meuse/Haute-Marne Underground Research Laboratory. *J. of Rock Mech. and Geotech.* Eng. **5** 221–230 (2013).
20. Zartman, G. D., Liu, H., Akdim, B., Pachter, R. & Heinz, H. Nanoscale Tensile, Shear, and Failure Properties of Layered Silicates as a Function of Cation Density and Stress. *J. Phys. Chem. C* **114**, 1763–1772 (2010).
21. Simmons, G. & Wang, H. *Single Crystal Elastic Constants and Calculated Aggregate Properties: A Handbook.* (Cambridge Press, 1971).
22. Sachse, W. & Ruoff, A. L. Elastic Moduli of Precompressed Pyrophyllite Used in Ultra-high Pressure Research. *J. Appl. Phys.* **46**, 3725–3730 (1975).
23. Vaughan, M. T. & Guggenheim, S. Elasticity of muscovite and its relationship to crystal structure. *J. Geophys. Res.* **91**, 4657–4664 (1986).
24. McNeil, L. E. & Grimsditch, M. Elastic moduli of muscovite mica. *J. Phys.: Condens. Matter* **5**, 1681–1690 (1993).
25. Faust, J. & Knitte, E. The equation of state, amorphization, and high-pressure phase diagram of muscovite. *J. Geophys. Res.* **99**, 19785–19792 (1994).
26. Catti, M., Ferraris, G., Hull, S. & Pavese, A. Powder neutron diffraction study of $2M_1$ muscovite at room pressure and at 2 GPa. *Eur. J. Mineral.* **6**, 171–178 (1994).
27. Habelitz, S. *et al.* Mechanical properties of oriented mica glass ceramic. *J. Non-Cryst. Solids* **220**, 291–298 (1997).
28. Pavese, A., Ferraris, G., Pischedda, V. & Mezouar, M. Synchrotron powder diffraction study of phengite 3T from the Dora-Maira massif: P - V - T equation of state and petrological consequences. *Phys. Chem. Miner.* **26**, 460–467 (1999).
29. Smyth, J. R. *et al.* Crystal structures and compressibilities of synthetic $2M_1$ and 3T phengite micas. *Eur. J. Mineral.* **12**, 955–963 (2000).
30. Pawley, A. R., Clark, S. M. & Chinnery, N. Equation of state measurements of chlorite, pyrophyllite, and talc. *J. Am. Mineral.* **87**, 1172–1182 (2002).
31. Sekkal, W., Zaoui, A. & Shahrour, H. Stability and adhesion of calcite/montmorillonite assembly. Amer. Miner. (2014) (in press). http://www.minsocam.org/MSA/Ammin/AM_Preprints.html).
32. Geissbuhler, P. *et al.* Three dimensional structure of the calcite-water interface by surface X-ray scattering. *Surf. Sci.* **573**, 191–203 (2004).
33. Stipp, S. L. S. Where the Bulk Terminates: Experimental evidence for restructuring, chemibonded OH- and H+, adsorbed water and hydrocarbons on calcite surfaces. *Mol. Simul.* **28**, 497–516 (2002).
34. Morse, J. W., Arvidson, R. S. & Luttge, A. Calcium carbonate formation and dissolution. *Chem. Rev.* **107**, 342–381 (2007).
35. Raiteri, P. & Gale, J. D. Water Is the Key to Nonclassical Nucleation of Amorphous Calcium Carbonate. *J. Am. Chem. Soc.* **132**, 17623–17634 (2010).
36. Raiteri, P., Gale, J. D., Quigley, D. & Rodger, P. M. Derivation of an Accurate Force-Field for Simulating the Growth of Calcium Carbonate from Aqueous Solution: A New Model for the Calcite-Water Interface. *J. Phys. Chem. C* **114**, 5997–6010 (2010).
37. Cygan, R. T., Liang, J.-J. & Kalinichev, A. G. Molecular Models of Hydroxide, Oxyhydroxide, and Clay Phases and the Development of a General Force Field. *J. Phys. Chem. B.* **108**, 1255–1266 (2004).
38. Zheng, Y., Zaoui, A. & Pasteau, A. Interactions between portions of clay with various contacts and subjected to specific environmental conditions. *Appl. Surf. Sci.* **292 C**, 311–318 (2014).
39. Yang, W. & Zaoui, A. Uranyl Adsorption on (001) surfaces of Kaolinite: A Molecular Dynamics Study. *Appl. Clay Sci.* **80–81**, 98–106 (2013).
40. Benazzouz, B. K., Zaoui, A. & Belonoshko, A. B. Determination of the Melting temperature of Kaolinite by means of the Z-method. *Am. Miner.* **98**, 1881–1885 (2013).
41. Zheng, Y. & Zaoui, A. Temperature Effects on the Diffusion of Water and Monovalent Counterions in the Hydrated Montmorillonite. *Physica A: Statistical Mechanisms and its Applications* **392**, 5994–6001 (2013).
42. Yang, W. & Zaoui, A. Behind Adhesion of Uranyl onto Montmorillonite Surface: A Molecular Dynamics Study. *J. of Hazard. Mat.* **261**, 224–234 (2013).
43. Benazzouz, B. K. & Zaoui, A. Thermal behaviour and superheating temperature of Kaolinite from molecular dynamics. *Appl. Clay Sci.* **58**, 44–51 (2012).
44. Benazzouz, B. K. & Zaoui, A. Thermal behaviour and superheating temperature of Kaolinite from molecular dynamics. *Appl. Clay Sci.* **58**, 44–51 (2012).
45. Benazzouz, B. K. & Zaoui, A. Phase diagram of kaolinite from Molecular Dynamics calculations. *Physica B: Condens. Mat.* **407**, 2462–2470 (2012).
46. Benazzouz, B. K. & Zaoui, A. A Nanoscale Simulation Study of the Elastic Behaviour in Kaolinite clay under pressure. *Mat. Chem. and Phys.* **132**, 880–888 (2012).
47. Zheng, Y. & Zaoui, A. How water and counterions diffuse into the hydrated montmorillonite. *Solid State Ionics* **203**, 80–85 (2011).
48. Zheng, Y., Zaoui, A. & Shahrour, I. A theoretical Study of Swelling and Shrinking of Hydrated Wyoming Montmorillonite. *Appl. Clay Sci.* **51**, 177–181 (2011).
49. Zheng, Y., Zaoui, A. & Shahrour, I. Evolution of the interlayer space of hydrated montmorillonite as a function of temperature. *Amer. Miner.* **95**, 1493–1499 (2010).
50. Xiao, S., Edwards, S. A. & Gräter, F. A New Transferable Forcefield for Simulating the Mechanics of $CaCO_3$ Crystals. *J. of Phys. Chem. C.* **115**, 20067–20075 (2011).
51. Sekkal, W. & Zaoui, A. Nanoscale analysis of the morphology and surface stability of calcium carbonate polymorphs. *Nature -Scientific Reports* **3**, 1587 (2013).
52. Jorgensen, W., Chandrasekhar, J., Madura, J. D., Impey, R. W. & Klein, M. L. Comparison of simple potential functions for simulating liquid water. *The J. of Chem. Phys.* **79**, 926–935 (1983).
53. Guillot, B. & Sator, N. Carbon dioxide in silicate melts: A molecular dynamics simulation study. *Geoch. & Cosmoch. Acta* **75**, 1829–1857 (2011).

Acknowelegments

The authors would like to thank the National Radioactive Waste Management Agency (ANDRA) for financial support. The authors are grateful to Dr F. Plas, A. Pasteau and J.C. Robinet for valuable discussions.

Author contributions

A.Z. conceived and designed the study. W.S. performed the theoretical studies and simulations. W.S. and A.Z. analysed and discussed the results. W.S. and A.Z. wrote the manuscript. All authors discussed the conceptual and practical implications of the method at all stages.

Additional information

Competing financial interests: The authors declare no competing financial interests.

How to cite this article: Zaoui, A. & Sekkal, W. Can clays ensure nuclear waste repositories? *Sci. Rep.* **5**, 8815; DOI:10.1038/srep08815 (2015).